tvst

https://doi.org/10.1167/tvst.8.4.12

Article

# Diagnostic Ability of Macular Vessel Density in the Ganglion Cell–Inner Plexiform Layer on Optical Coherence Tomographic Angiography for Glaucoma

Jonghoon Shin[1,2], Jeong Min Kwon[1,2], Su Hwan Park[1,2], Je Hyun Seo[3], and Jae Ho Jung[4]

[1] Department of Ophthalmology, College of Medicine, Pusan National University Yangsan Hospital, Yangsan, South Korea
[2] Department of Ophthalmology, Research Institute for Convergence of Biomedical Science and Technology, Pusan National University Yangsan Hospital, Yangsan, South Korea
[3] Department of Ophthalmology, Veterans Medical Research Institute, Seoul, Korea
[4] Department of Ophthalmology, Seoul National University College of Medicine, Seoul, South Korea

**Correspondence:** Jae Ho Jung, Department of Ophthalmology, Seoul National University Hospital, 101 Daehak-ro, Jongno-gu, Seoul, 03080, South Korea. e-mail: jaeho.jung@snu.ac.kr

**Received:** 15 February 2019
**Accepted:** 25 May 2019
**Published:** 30 July 2019

**Keywords:** ganglion cell–inner plexiform layer; glaucoma; macular vessel density; optical coherence tomographic angiography

**Citation:** Shin J, Kwon JM, Park SH, Seo JH, Jung JH. Diagnostic ability of macular vessel density in the ganglion cell–inner plexiform layer on optical coherence tomographic angiography for glaucoma. Trans Vis Sci Tech. 2019;8(4):12, https://doi.org/10.1167/tvst.8.4.12


**Purpose:** The purpose of this study was to analyze the macular vessel density layer-by-layer and compare the diagnostic value of each in diagnosing glaucoma.

**Methods:** This was a prospective comparative cross-sectional study, and the setting was glaucoma referral practice. The study participants were patients with primary open-angle glaucoma undergoing treatment with drugs, and age-matched normal controls who visited our clinic for regular eye examinations for refractive errors. All participants were investigated using macular optical coherence tomographic angiography, fundus photography, and 24-2 visual field (VF) testing. Average vessel densities in the retinal nerve fiber–ganglion cell–inner plexiform layer (IPL), retinal nerve fiber–ganglion cell layer (GCL), retinal nerve fiber layer (RNFL), ganglion cell–IPL, GCL, and IPL segments on optical coherence tomographic angiography.

**Results:** Fifty-eight glaucomatous eyes of 58 participants and 52 healthy eyes of 52 normal subjects were included in the study. The average vessel densities of all segments, except the RNFL in the glaucoma group, were significantly lower than that in normal subjects. The average vessel density in the ganglion cell–IPL showed the highest correlation with the mean deviation and VF index of the VF ($r = 0.515$ and 0.538, respectively) and the best area under receiver operating characteristic curve to discriminate between patients with glaucoma and patients with normal eyes (0.750).

**Conclusions:** The present study demonstrated that macular vessel density in the ganglion cell–IPL has a higher diagnostic ability and better correlation with functional damage in glaucoma than that in the superficial vascular plexus.

**Translational Relevance:** These findings suggest that the macular vessel density in the ganglion cell–inner plexiform layer is better than that in the conventional superficial vascular plexus for detecting glaucoma.

## Introduction

The development of optical coherence tomography angiography (OCTA) has enabled noninvasive measurements of vascular changes in the retinal layers, and this new tool has been increasingly used in retinal diseases and glaucoma.[1–4] Several previous studies have investigated the vessel density in the peripapillary area or parafoveal region with OCTA in patients with glaucoma.[5–9] Some of these studies have shown that the abnormal vessel density in OCTA has a significant association with glaucomatous optic nerve damage, although it has been controversial whether these abnormal vascular density in glaucoma are the primary cause of the disorder or secondary changes due to the disorder.[7,8,10]

Chung et al.[1] and Rao et al.[11] showed that the

diagnostic abilities of vascular densities in the peripapillary and macular regions measured using OCTA in patients with glaucoma were significantly lower than those using structural measurements of the peripapillary retinal nerve fiber layer (RNFL) obtained by OCT; this study speculated that the automatic software provided by the OCTA manufacturer might be one of the factors responsible for the low diagnostic abilities of the vessel parameters as measured by OCTA in glaucoma. In fact, the OCTA superficial image shows the superficial capillary network around the fovea. It extends from the internal limiting membrane (ILM) to 15.6 μm under the boundary between the inner plexiform layer (IPL) and inner nuclear layer (INL). This layer included the ILM, RNFL, ganglion cell layer (GCL), IPL, and the part of INL.[11] We would like to highlight that merged multiple layer analysis from the previous study may not reflect specific vessel density of each layer and/or interfere original vessel density of each layer. Therefore, there was limitation and inaccuracy for discovering the correlation between vessel OCTA parameters and glaucoma diagnosis.

However, with the recent developments in OCTA software, it is possible to segment the macular vessel density and to measure the vessel density layer-by-layer. Therefore, in this study, we analyzed the macular vessel density layer-by-layer and compared the diagnostic ability of each for detection of glaucoma.

## Material and Methods

This study was approved by the institutional review board (Pusan National University Yangsan Hospital, Yangsan, South Korea). After the purposes and procedures of the study had been fully explained, each patient gave consent to participate in the study. All testing was conducted in accordance with the tenets of the Declaration of Helsinki.

This was a prospective, cross-sectional, comparative study, and the present study was carried out in a glaucoma referral center. The study participants were primary open-angle glaucoma patients undergoing treatment with drugs, and age-matched normal controls who visited our clinic for regular eye examinations for refractive errors. Patients with open-angle glaucoma detected by gonioscopic examination and normal controls with no history of ocular diseases, intraocular pressure (IOP) $\leq$ 21 mm Hg, absence of a glaucomatous optic disc, and a normal visual field (VF) were included in the study. Glaucoma was defined as the following criteria: asymmetric cup-to-disc ratio $\geq$ 0.2, vertical cup-to-disc ratio $>$ 0.7, neural rim thinning, localized notching, disc hemorrhage, and RNFL defects with corresponding glaucomatous VF defects.[12–14] Subjects were excluded if they had best-corrected visual acuity (BCVA) less than 20/40, a refractive error outside the range of –6.0 to +3.0 diopters, astigmatism beyond ± 3.0 diopters, previous ocular trauma, ocular surgery or laser treatment, or a history of ocular or systemic disease that could affect the optic nerve or VF.

Each subject underwent a complete ophthalmologic examination that included BCVA measurements, slit-lamp examination, gonioscopy, IOP measurement with the Goldmann applanation tonometer, fundus examination, and stereo optic nerve evaluation with a 90-diopter lens. Red-free fundus photography using a nonmydriatic fundus camera (Canon CR-2, Canon, Tokyo, Japan), OCTA measurements using Topcon Atlantis (DRI OCT-1, Topcon, Tokyo, Japan), and automated VF examination using the Humphrey 740 Visual Field Analyzer (Carl Zeiss Meditec, Dublin, CA) were performed on all subjects. We defined glaucomatous VFs based on the presence of two of the following criteria: (1) an abnormal glaucoma hemi-field test result (a borderline score was not considered abnormal); (2) three continuous nonedge points (allowing the two-step nasal edge points) with $P < 0.05$ on the total deviation plot, with at least one point having $P < 0.01$; (3) $P < 0.05$ for the pattern standard deviation (PSD) on the Swedish Interactive Threshold Algorithm (SITA) Standard test.

### OCTA Data Acquisition and Processing

Images were obtained using a DRI OCT Atlantis swept source-optical coherence tomography (SS-OCT) device (Topcon). SS-OCT uses infrared light with a wavelength of 1050 nm, which is longer than that of conventional spectral domain-optical coherence tomography (SD-OCT), at 100,000 axial scans (A scans) per second. This longer infrared light source has the advantage of deep signal penetration through the retina and choroid. Its axial and transversal resolutions in the tissue are 7 and 20 μm, respectively. Volumetric OCT scans were performed with $6 \times 6$ mm cubes. Each cube consisted of 320 clusters of four repeated two-dimensional transverse scans (B scans) centered on the fovea. We detected moving objects (mostly blood flow) by measuring intensity fluctuations from these repeatedly scanned OCT images. In this technique, called OCT angiography ratio analysis

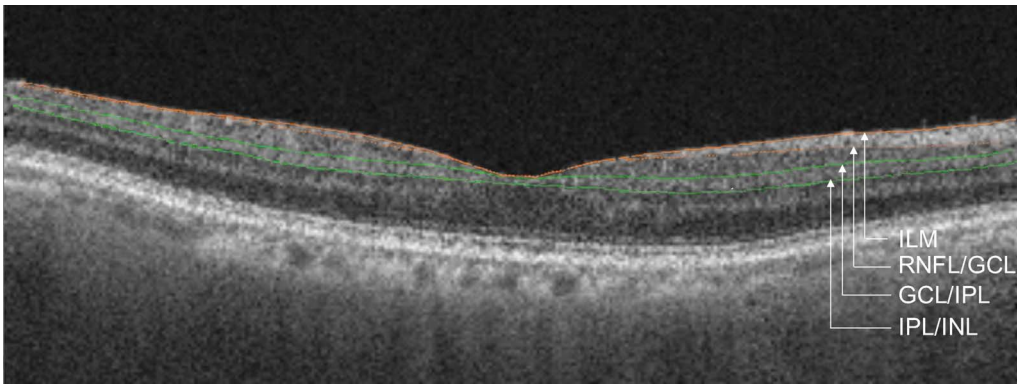


**Figure 1.** Division of the segmented parafoveal retinal layer using optical coherence tomographic angiography in a normal subject. The automated software demonstrated the four vessel density parameters in the 3 × 3 mm circular scan area, divided into the nasal, inferior, superior, and temporal sectors. In addition, since the automated program could also show the inner limiting membrane (*orange solid line*) and the boundaries between the RNFL and the GCL (*orange dot line*), between the GCL and the IPL (*upper green line*), and between the IPL and the INL (*lower green line*), we performed a segmented layer-by-layer analysis in the inner retinal layers.

(OCTARA), calculations are based on the ratio of the intensity values across points within one scan and identical points in repeated scans. We performed automated segmentation using OCT software to separate each layer of the retina. The en face images of the superficial capillary network were derived from an en face slab ranging from the ILM to the inner border of the INL. The automated segmentation software for Atlantis SS-OCT identified four different retinal boundaries: inner limiting membrane, boundaries between the RNFL and the GCL, the GCL and the IPL, and the IPL and the INL. The vessel density in each RNFL, GCL, and IPL layer was obtained. In addition, we investigate the inner, outer, and both vessel densities, centered on the GCL by adjusting auto-segmented layers. We could obtain various vessel densities values based on single retina layer and two or more overlapped retina layer, and finally, we could evaluate the six-layer vessel densities, respectively: (1) RNF–GC–IPL, (2) RNF–GCL, (3) RNFL, (4) GC–IPL, (5) GCL, and (6) IPL segments.

The macular vessel density map was analyzed over a 3 × 3 mm annulus area centered on the macula. The parafoveal region was also divided into four sectors, namely, the nasal, inferior, superior, and temporal sectors, and the average vessel density of each layer was obtained by averaging the measurements of the four sectors (Fig. 1).

### Statistical Analysis

The assumption of data normality was tested using the Kolmogorov-Smirnov test. The Student's *t*-test or the Mann-Whitney *U* test was used to compare continuous data. One-way analysis of variance test was used for comparison of OCTA vessel density and OCT measurements among the normal control, mild, and moderate-to-severe glaucoma group. Multiple comparisons with Bonferroni adjustments were used for pairwise comparisons. $P$ values $< 0.05$ were considered statistically significant. The Pearson-Spearman correlation test was used to investigate the correlation between the VF parameters and the vessel density of each layer. Receiver operating characteristic (ROC) curves were used to describe the ability of vessel density obtained from OCTA to differentiate glaucoma from normal controls. Area under the ROC curve (AUROC) was calculated to assess the diagnostic accuracy of each measurement. An AUROC of 1.0 represented perfect discrimination, whereas an AUROC of 0.5 represented chance discrimination. The method described by DeLong et al.[15] was applied to compare the AUROCs. Statistical analyses were performed with SPSS for Windows 21.0 (SPSS, Inc., Chicago, IL) and Medcalc version 10.0 (Medcalc Software; Ostend, Mariakerke, Belgium).

## Results

This study enrolled 58 glaucomatous eyes of 58 participants and 52 healthy eyes of 52 normal subjects. The demographic data of the subjects are summarized in Table 1. Mean deviation (MD), PSD, and VF index (VFI) in the glaucoma group were lower than those in normal subjects. There were no significant differences regarding other demographic and ocular factors including age, sex, spherical equivalent, corneal thickness, and history of diabetes

**Table 1.** Demographics and Ocular Characteristics of Participants With Primary Open Angle Glaucoma and Normal Subjects

| | Glaucoma (58 Eyes) | Normal Subjects (52 Eyes) | *P* |
|---|---|---|---|
| Age, mean ± SD (years) | 55.32 ± 15.37 | 57.27 ± 17.35 | 0.495 |
| Sex (M/F) | 38/20 | 27/25 | 0.148 |
| Spherical equivalent, mean ± SD (D) | −1.05 ± 2.45 | −0.34 ± 2.37 | 0.123 |
| Central corneal thickness, mean ± SD (μm) | 552.34 ± 40.05 | 555.81 ± 35.61 | 0.675 |
| Diabetes mellitus (yes/no) | 11/47 | 10/42 | 0.972 |
| Hypertension (yes/no) | 13/45 | 6/46 | 0.132 |
| MD, mean ± SD (dB) | −11.03 ± 8.62 | −0.40 ± 0.97 | <0.001 |
| PSD, mean ± SD (dB) | 9.98 ± 4.55 | 1.53 ± 0.43 | <0.001 |
| VFI, mean ± SD (%) | 64.94 ± 27.11 | 99.01 ± 1.03 | <0.001 |

M, Male; F, Female.

mellitus and systemic hypertension between the two groups.

The OCTA vessel density parameters in the RNF–GC–IPL, RNF–GCL, RNFL, GC–IPL, GCL, and IPL segments, and OCT measurements in peripapillary and parafoveal area in patients with glaucoma and normal subjects are presented in Table 2. Significant differences among mild glaucoma, moderate-to-severe glaucoma, and normal controls were found in vessel density in all segments, the peripapillary RNFL thickness, and macular thickness in GC-IPL and RNF-GC-IPL. The average vessel densities of all segments, except RNFL in the glaucoma group, were significantly lower than that in normal subjects. Conversely, the average vessel density in the RNFL in the glaucoma group was significantly higher than that in normal subjects ($P < 0.001$).

Correlation analyses between the OCTA vessel density parameters and functional parameters (MD, PSD, and VFI) in patients with glaucoma are provided in Table 3. There was a significantly positive correlation between the MD and vessel density in the RNF–GC–IPL, GCL–IPL, and IPL ($r = 0.294$, 0.515, and 0.300, respectively) and between the VFI and vessel density in the RNF–GC–IPL, GC–IPL, and IPL ($r = 0.299$, 0.538, and 0.364, respectively).

The diagnostic abilities of the OCTA vessel density parameters in the glaucoma group and normal subjects are shown in Figure 2. The average vessel density in the GC-IPL had the best AUROC in terms of discriminating patients with glaucoma from patients with normal eyes, followed by that in the RNF–GC–IPL, IPL, GCL, and RNF-GCL (0.750, 0.708, 0.706, 0.679, and 0.626, respectively). In addition, the AUROC for vessel density in the GC-IPL was significantly greater than for vessel density in the other segments; RNF-GC-IPL, IPL, GCL, and RNF-GCL ($P = 0.025$, 0.041, 0.042, 0.001, respectively). On the other hand, the AUROC for vessel density in RNF-GCL was significantly lower than for the vessel density in RNF-GC-IPL, IPL, and GCL ($P = 0.019$, 0.039, 0.003, respectively).

## Discussion

The present study found that the OCTA vessel density was significantly lower in all segmented areas, except the RNFL layer, in eyes with glaucoma than in normal subjects. In the glaucomatous eye, the OCTA vessel density in RNF–GC–IPL, GC–IPL, and IPL had significant correlation with the MD and VFI as measured on the HVF. Moreover, not only did the OCTA vessel density in GC–IPL show the highest correlation with functional parameters, but it also had the greatest diagnostic ability among the vessel densities in the various segments as measured by OCTA in terms of discriminating primary open-angle glaucoma patients from normal subjects.

Rao et al.[11] compared the diagnostic abilities of OCTA vessel density of the optic nerve head and the peripapillary and macular area in glaucomatous eyes; it was observed that the area under the curve (AUC) of the average vessel densities measured by OCTA within the optic nerve head and the peripapillary and macular regions were 0.77, 0.85, and 0.70, respectively.[11] The study by Chung et al.[1] also showed the average vessel densities in the optic nerve head and the peripapillary and macular areas to be 0.566, 0.807, and 0.651, respectively; moreover, in the analysis of the glaucoma stage, the OCTA vessel density in the macula showed the best diagnostic ability at the severe stage of glaucoma with an AUC of 0.773.[1]

**Table 2.** Average Vessel Density (Range) Obtained by Optical Coherence Tomographic Angiography and Structural Parameters Measured by OCT in Primary Open Angle Glaucoma and Normal Subjects

| | Mild Glaucoma (20 Eyes) | Moderate-to-Severe Glaucoma (38 Eyes) | Normal Subjects (52 Eyes) |
|---|---|---|---|
| Average vessel density in RNF-GC-IPL | 43.17 (42.03–44.28) | 42.04 (41.11–42.98) | 44.17 (43.68–44.65) |
| Average vessel density in RNF-GCL | 41.11 (40.33–41.95) | 40.55 (39.54–41.57) | 41.78 (41.27–42.32) |
| Average vessel density in RNFL | 44.88 (43.29–46.50) | 46.64 (44.60–48.68) | 43.04 (42.48–43.67) |
| Average vessel density in GC-IPL | 43.49 (42.26–44.63) | 41.76 (40.92–42.54) | 44.65 (44.17–45.13) |
| Average vessel density in GCL | 41.12 (40.20–42.08) | 40.26 (39.30–41.18) | 42.05 (41.58–42.55) |
| Average vessel density in IPL | 43.54 (42.40–44.65) | 41.98 (41.16–42.71) | 44.25 (43.80–44.67) |
| Average peripapillary RNFL thickness (μm) | 72.38 (62.71–81.27) | 56.10 (50.77–61.73) | 106.90 (104.09–109.94) |
| Average thickness in GC-IPL (μm) | 72.97 (67.45–78.67) | 60.65 (56.08–65.63) | 87.41 (85.09–89.67) |
| Average thickness in RNF-GC-IPL (μm) | 98.05 (91.61–104.45) | 85.48 (80.80–90.56) | 115.41 (112.08–119.26) |

**Table 2.** Extended

| | *P* Value | | | |
|---|---|---|---|---|
| | Total | Mild vs. Normal | Moderate to Severe vs. Normal | Mild vs. Moderate to Severe |
| Average vessel density in RNF-GC-IPL | <0.001 | 0.356 | <0.001 | 0.005 |
| Average vessel density in RNF-GCL | 0.045 | 0.814 | 0.035 | 0.455 |
| Average vessel density in RNFL | <0.001 | 0.178 | <0.001 | 0.139 |
| Average vessel density in GC-IPL | <0.001 | 0.167 | <0.001 | 0.002 |
| Average vessel density in GCL | <0.001 | 0.379 | <0.001 | 0.344 |
| Average vessel density in IPL | <0.001 | 0.551 | <0.001 | 0.005 |
| Average peripapillary RNFL thickness (μm) | <0.001 | <0.001 | <0.001 | 0.002 |
| Average thickness in GC-IPL (μm) | <0.001 | <0.001 | <0.001 | 0.001 |
| Average thickness in RNF-GC-IPL (μm) | <0.001 | <0.001 | <0.001 | 0.005 |

However, in these previous studies, the segment used for the macular vessel density analysis was the superficial vascular plexus defined as the area extending from the ILM to the IPL.[1,11] Although previous studies have demonstrated the ability of macular vessel density on OCTA to diagnose glaucoma, to date, there are no reports comparing the macular vessel density in various layers from the RNFL to the IPL. In fact, analysis of the average OCTA vessel density in the macula in the present study showed that the OCTA vessel density in the GC–IPL had relatively better AUC than that in the RNF-GC-IPL in the present study as well as compared with previous studies.

The present study revealed that the OCTA vessel density in the RNFL in eyes with glaucoma was significantly higher than that in normal subjects. These results may be associated with the variability of the automated measurements of macular RNFL thickness. Kotera et al.[16] suggested that this variability partially led to failure of accurately detecting the outer boundary of the macular RNFL in some sectors, and macular RNFL thickness in glaucoma patients tended to show higher variability than in normal controls. In the present study, when the glaucoma eyes were classified as mild (MD > −6 dB) or moderate to severe (MD < −6 dB), the difference of VD in RNFL between normal and mild glaucoma was not statistically significant, but the difference between normal and moderate-to-severe glaucoma was statistically significant. As the glaucomatous damage became more severe, RNFL thickness was thinner than that in normal, and then this segmentation error in severe stage could be more common than

**Table 3.** Pearson Correlation Coefficients Between Average Vessel Density and VF Parameters Including MD and PSD

| | MD (dB) | PSD (dB) | VFI (%) |
|---|---|---|---|
| Average vessel density in RNF-GC-IPL | | | |
| *r* | 0.294 | −0.224 | 0.299 |
| *P* | 0.029 | 0.100 | 0.037 |
| Average vessel density in RNF-GCL | | | |
| *r* | 0.031 | −0.127 | 0.023 |
| *P* | 0.823 | 0.356 | 0.877 |
| Average vessel density in RNFL | | | |
| *r* | −0.211 | 0.048 | −0.250 |
| *P* | 0.122 | 0.729 | 0.084 |
| Average vessel density in GC-IPL | | | |
| *r* | 0.515 | −0.264 | 0.538 |
| *P* | <0.001 | 0.052 | <0.001 |
| Average vessel density in GCL | | | |
| *r* | 0.054 | −0.155 | 0.120 |
| *P* | 0.697 | 0.259 | 0.411 |
| Average vessel density in IPL | | | |
| *r* | 0.300 | −0.116 | 0.364 |
| *P* | 0.026 | 0.397 | 0.010 |

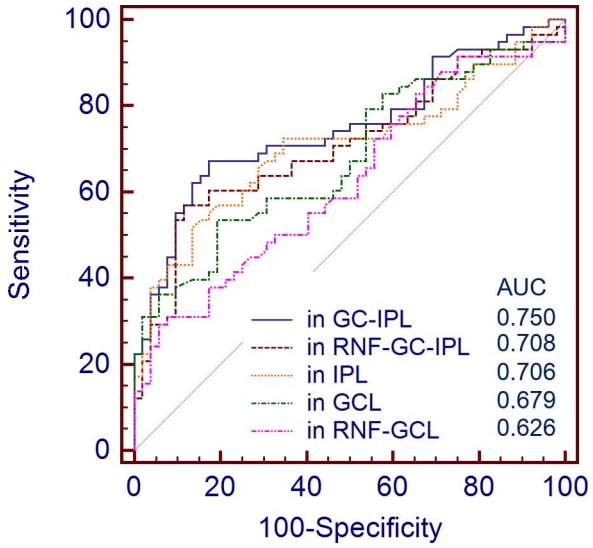


**Figure 2.** ROC curves for vessel density parameters measured by optical coherence tomographic angiography.

in normal or glaucoma suspect. This may be the reason why RNFL thinning in glaucoma is associated with segmentation error in the OCT scanning of the macular area.

In addition, histological studies in glaucoma patients have shown pathological changes in the inner retina, including the RNFL, GCL, and IPL, where ganglion cells are distributed.[17–19] Further, a decreased GC–IPL thickness on macular OCT and decreased retinal ganglion cell (RGC) function in pattern electroretinography have been detected in glaucoma patients.[20,21] These glaucomatous changes in the RGC might be associated with modulation of the retinal glial cells, which contribute to the maintenance of the normal function of the ganglion cell by controlling the extracellular environment (including the supply of metabolites) and the vasculature.[22,23] Recently, it has been shown that the various parameters measured by OCTA can provide evidence of the impairment of the vascular components related with ganglion cell dysfunction in glaucoma.[8,24]

In our study, we observed that the significant reduction of OCTA vessel density in the GC-IPL in the patients with glaucoma except for RNFL of the superficial vascular plexus. These results show clinical usefulness of OCTA measurements for the diagnosis of glaucoma. The OCTA vessel densities in the RNF–GC–IPL, GC–IPL, and IPL had a significant correlation with the functional parameters, MD and VFI, in the present study. These results agree with those of previous studies.[8,25] Yarmohammadi et al.[8] suggested that the vascular abnormalities detected by OCTA may better reflect the dysfunctional status of the RGCs than structural measurements alone in glaucomatous eyes. In addition, the highest correlation of the vessel density of the GC–IPL layer among all the inner layers with the functional parameters observed in the present study may be because it has been observed that abnormalities in the RGC soma and dendrites are detected earlier than axonal loss in the early stage of glaucoma.[26,27]

In the analysis of the parafoveal vessel density using OCTA, the present study also revealed that the vessel density in the superficial vascular plexus representing the RNF–GC–IPL had a lower ability to diagnose glaucoma than the peripapillary vessel density used in other studies,[11,16] and therefore, it can be considered that the clinical usefulness of macular OCTA in glaucoma is less than that of the peripap-

illary parameters in the OCTA. However, the present study investigated the vessel density in the various segments through segmentation of the RNFL, GCL, and IPL included in the superficial vascular plexus and found that the OCTA vessel density in the GC-IPL had a greater diagnostic ability to discriminate between glaucomatous and normal eyes compared with the other segments.

There are some limitations in this study. First, since the automated analysis maneuver of vessel density provided by the OCTA machine is based on the Early Treatment Diabetic Retinopathy Study (ETDRS) map, which does not have horizontal borders along the horizontal meridian, the present study could not evaluate the analysis of the sectorial vessel densities in various areas. Second, it was difficult to compare the diagnostic ability of vessel densities of the parafoveal region and the peripapillary area because the software could not measure the vessel density in the peripapillary area. Third, the present study did not measure the systolic, diastolic, and mean blood pressure and evaluate the duration of the hypertension, and the antihypertensive or antidiabetic drugs used in all the participants, and therefore, the effect of systemic drugs on the vascular density in the macula cannot be excluded in spite of the relatively low association observed between blood pressure and retinal vessel density in OCTA in a previous study.[9]

In conclusion, the present study demonstrated that macular vessel density in the GC–IPL has a higher diagnostic ability and better correlation with functional damage in glaucoma than that in the superficial vascular plexus, which is used conventionally. Further studies are needed to improve the diagnostic ability of OCTA using vessel density in the GC–IPL to detect glaucoma.

## Acknowledgments

Design of the study (J. Shin, J.H. Seo, J.H. Jung); conduct of the study (J. Shin, J.H. Seo); data collection and management (S.H. Park, J. Shin); analysis and interpretation of data (J.H. Seo, J.H. Jung); preparation, review, and approval of the manuscript (J. Shin, J.M. Kwon, S.H. Park, J.H. Seo, J.H. Jung).

J. Shin had full access to all the data in the study and takes responsibility for the integrity of the data and the accuracy of the data analysis.

Disclosure: **J. Shin**, None; **J.M. Kwon**, None; **S.H. Park**, None; **J.H. Seo**, None; **J.H. Jung**, None

## References

1. Chung JK, Hwang YH, Wi JM, Kim M, Jung JJ. Glaucoma diagnostic ability of the optical coherence tomography angiography vessel density parameters. *Curr Eye Res*. 2017;42:1458–1467.
2. Wan KH, Leung CKS. Optical coherence tomography angiography in glaucoma: a mini-review. *F1000Res*. 2017;6:1686.
3. Rao HL, Pradhan ZS, Weinreb RN, et al. Regional comparisons of optical coherence tomography angiography vessel density in primary open-angle glaucoma. *Am J Ophthalmol*. 2016; 171:75–83.
4. Akagi T, Iida Y, Nakanishi H, et al. Microvascular density in glaucomatous eyes with hemifield visual field defects: an optical coherence tomography angiography study. *Am J Ophthalmol*. 2016;168:237–249.
5. Chen CL, Zhang A, Bojikian KD, et al. Peripapillary retinal nerve fiber layer vascular microcirculation in glaucoma using optical coherence tomography–based microangiography. *Invest Ophthalmol Vis Sci*. 2016;57:475–485.
6. Jia Y, Wei E, Wang X, et al. Optical coherence tomography angiography of optic disc perfusion in glaucoma. *Ophthalmology*. 2014;121:1322–1332.
7. Lee EJ, Lee KM, Lee SH, Kim TW. OCT angiography of the peripapillary retina in primary open-angle glaucoma. *Invest Ophthalmol Vis Sci*. 2016;57:6265–6270.
8. Yarmohammadi A, Zangwill LM, Diniz-Filho A, et al. Peripapillary and macular vessel density in patients with glaucoma and single-hemifield visual field defect. *Ophthalmology*. 2017;124: 709–719.
9. Liu L, Jia Y, Takusagawa HL, et al. Optical coherence tomography angiography of the peripapillary retina in glaucoma. *JAMA Ophthalmol*. 2015;133:1045–1052.
10. Chen CL, Bojikian KD, Wen JC, et al. Peripapillary retinal nerve fiber layer vascular microcirculation in eyes with glaucoma and single-hemifield visual field loss. *JAMA Ophthalmol*. 2017;135:461–468.
11. Rao HL, Pradhan ZS, Weinreb RN, et al. A comparison of the diagnostic ability of vessel

density and structural measurements of optical coherence tomography in primary open angle glaucoma. *PLoS One*. 2017;12:e0173930.
12. Leske MC, Connell AM, Schachat AP, Hyman L. The Barbados eye study. Prevalence of open angle glaucoma. *Arch Ophthalmol*. 1994;112:821–829.
13. Wolfs RC, Borger PH, Ramrattan RS, et al. Changing views on open-angle glaucoma: definitions and prevalences: The Rotterdam Study. *Invest Ophthalmol Vis Sci*. 2000;41:3309–3321.
14. Anderson DR. *Automated Static Perimetry*. St Louis, MO: Mosby-Year Book; 1992:123.
15. DeLong ER, DeLong DM, Clarke-Pearson DL. Comparing the areas under two or more correlated receiver operating characteristic curves: a nonparametric approach. *Biometrics*. 1988;44: 837–845.
16. Kotera Y, Hangai M, Hirose F, Mori S, Yoshimura N. Three-dimensional imaging of macular inner structures in glaucoma by using spectral-domain optical coherence tomography. *Invest Ophthalmol Vis Sci*. 2011;52:1412–1421.
17. Markoulli M, Duong TB, Lin M, Papas E. Imaging the tear film: a comparison between the subjective Keeler Tearscope-Plus™ and the objective Oculus® Keratograph 5M and Lipi-View® Interferometer. *Curr Eye Res*. 2018;43: 155–162.
18. Choi JH, Law MY, Chien CB, Link BA, Wong ROL. In vivo development of dendritic orientation in wild-type and mislocalized retinal ganglion cells. *Neural Dev*. 2010;5:29.
19. Kim EK, Park HYL, Park CK. Segmented inner plexiform layer thickness as a potential biomarker to evaluate open-angle glaucoma: dendritic degeneration of retinal ganglion cell. *PLoS One*. 2017;12:e0182404.
20. Raza AS, Cho J, de Moraes CG, et al. Retinal ganglion cell layer thickness and local visual field sensitivity in glaucoma. *Arch Ophthalmol*. 2011; 129:1529–1536.
21. Hood DC, Raza AS, de Moraes CG, Liebmann JM, Ritch R. Glaucomatous damage of the macula. *Prog Retin Eye Res*. 2013;32:1–21.
22. Tezel G, Wax MB. Glial modulation of retinal ganglion cell death in glaucoma. *J Glaucoma*. 2003;12:63–68.
23. Osborne NN, Melena J, Chidlow G, Wood JPM. A hypothesis to explain ganglion cell death caused by vascular insults at the optic nerve head: possible implication for the treatment of glaucoma. *Br J Ophthalmol*. 2001;85:1252–1259.
24. Suh MH, Zangwill LM, Manalastas PIC, et al. Optical coherence tomography angiography vessel density in glaucomatous eyes with focal lamina cribrosa defects. *Ophthalmology*. 2016; 123:2309–2317.
25. Sehi M, Goharian I, Konduru R, et al. Retinal blood flow in glaucomatous eyes with single-hemifield damage. *Ophthalmology*. 2014;121:750–758.
26. El-Danaf RN, Huberman AD. Characteristic patterns of dendritic remodeling in early-stage glaucoma: evidence from genetically identified retinal ganglion cell types. *J Neurosci*. 2015;35: 2329–2343.
27. Mayama C, Saito H, Hirasawa H, et al. Diagnosis of early-stage glaucoma by grid-wise macular inner retinal layer thickness measurement and effect of compensation of disc-fovea inclination. *Invest Ophthalmol Vis Sci*. 2015;56: 5681–5690.